A&A manuscript no. (will be inserted by hand later)	ASTRONOMY
Your thesaurus codes are: 06 (02.01.2; 02.08.1; 02.09.1; 02.19.1; 08.02.1; 13.25.5)	ASTROPHYSICS

Entropic-Acoustic instability in shocked accretion flows

T. Foglizzo^{1*} and M. Tagger^{1**}

Service d'Astrophysique, CEA/DSM/DAPNIA (CNRS URA 2052), CE-Saclay, 91191 Gif-sur-Yvette, France

Received 15 May 2000; accepted 7 September 2000

Abstract. A new instability mechanism is described in accretion flows where the gas is accelerated from a stationary shock to a sonic surface. The instability is based on a cycle of acoustic and entropic waves in this subsonic region of the flow. When advected adiabatically inward, entropy perturbations trigger acoustic waves propagating outward. If a shock is present at the outer boundary, acoustic waves reaching the shock produce new entropy perturbations, thus creating an entropic-acoustic cycle between the shock and the sonic surface. The interplay of acoustic and entropy perturbations is estimated analytically using a simplified model based on the compact nozzle approximation. According to this model, the entropic-acoustic cycle is unstable if the sound speed at the sonic surface significantly exceeds the sound speed immediately after the shock. The growth rate scales like the inverse of the advection time from the outer shock to the sonic point. The frequency of the most unstable perturbations is comparable to the refraction cutoff, defined as the frequency below which acoustic waves propagating inward are significantly refracted outward. This generic mechanism should occur in Bondi-Hoyle-Lyttleton accretion, and also in shocked accretion discs.

Key words: Accretion, accretion disks – Hydrodynamics – Instabilities – Shock waves – Binaries: close – X-rays: stars

1. Introduction

Hydrodynamic instabilities in the process of accretion onto a compact star may help to understand the time variability of the emission from X-ray binaries. For example, the supersonic motion of a compact star in a uniform gas, first described by Hoyle & Lyttleton (1939), Bondi & Hoyle (1944), was later found to be unstable in numerical simulations (Matsuda et al. 1987, Fryxell & Taam 1988, Matsuda et al. 1992, Ruffert & Arnett 1994). In such flows,

 $Send\ off print\ requests\ to:$ T. Foglizzo

* e-mail: foglizzo@cea.fr ** e-mail: tagger@cea.fr

the gas captured by the accretor is first heated and decelerated to subsonic velocities through a shock, and then accelerated to supersonic velocities towards the accretor. Observationnal consequences of the instability were discussed by Taam et al. (1988), Livio (1992), De Kool & Anzer (1993). Nevertheless, this instability is still poorly understood even in its simplest formulation. A recent attempt by Foglizzo & Ruffert (1999) has led us to look in more detail at the interplay of acoustic and entropy waves in the subsonic flow between the bow shock and the accretor. We identify in the present paper an entropic-acoustic cycle: entropy perturbations advected with the flow trigger acoustic waves propagating back to the shock, where in turn they trigger new entropy perturbations. The linear stability of this cycle depends on the efficiencies of these two processes, measuring:

- (i) the amplitude of the pressure perturbations δp^- propagating against the stream, triggered by the advection of an entropy wave of amplitude δS_1 ,
- (ii) the amplitude of the entropy perturbation δS_2 triggered by the interaction of an acoustic wave δp^- with a stationary shock.

The entropic-acoustic cycle is a priori unstable if $\delta S_2 > \delta S_1$. As will be seen throughout this paper, a complete description of the entropic-acoustic instability requires to take into account acoustic waves δp^+ propagating with the stream, triggered by the interaction of δp^- with the shock and refracted out by the flow gradients.

Since such entropic-acoustic cycles may be present in astrophysical flows other than the Bondi-Hoyle-Lyttleton accretion, the present paper is dedicated to a description of this generic mechanism in its most general formulation. Similar entropic-acoustic cycles have been studied extensively in the context of jet nozzles, where the gravitational potential plays no role. In particular, the first process (i) is well known among the combustion community since the works of Candel (1972) and Marble (1973). A clear overview of the subject can be found in Marble & Candel (1977). An example of entropic-acoustic instability in nozzles is the ramjet 'rumble' instability studied by Abouseif, Keklak & Toong (1984), where the combustion zone plays the same role as the shock in the second pro-

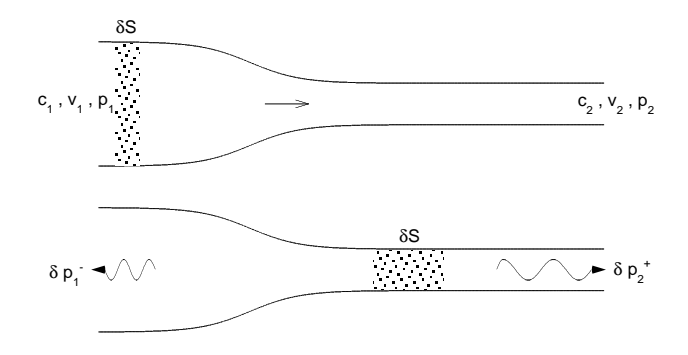


Fig. 1. Illustration of the release of acoustic energy by the advection of a localized perturbation of entropy in a nozzle

cess (ii).

The paper is organized as follows: in Sect. 2 we analyze the excitation of acoustic waves by the advection of entropy perturbations. The entropy perturbations produced by a sound wave reaching a shock are estimated in Sect. 3. These two processes are combined into a global mode in Sect. 4, where we characterize its spectrum of eigenfrequencies. Possible astrophysical applications are discussed in Sect. 5.

2. Acoustic energy released by the advection of entropy perturbations in an irrotational flow

2.1. Energy released by the advection of a localized perturbation of entropy

We wish to estimate the energy δE_{12} released by the advection of a perturbation δS of entropy into a gravitational potential, from a region I where the unperturbed velocity, sound speed and gravitational potential are v_1, c_1, Φ_1 to a region II closer to the accretor where their respective values are v_2, c_2, Φ_2 . These quantities are related through the conservation of the Bernoulli constant B in the unperturbed flow. Denoting by γ the adiabatic index of the gas, and by h its enthalpy,

$$B \equiv \frac{v^2}{2} + h + \Phi, \tag{1}$$

$$h \equiv \frac{c^2}{\gamma - 1}.\tag{2}$$

A direct calculation of δE_{12} is possible when the unperturbed flow is uniform before and after the region of convergence, so that the entropy perturbation has enough time to reach a pressure equilibrium with the surrounding gas (see Fig. 1). Let $m + \delta m$ be the mass of the gas with a perturbed entropy $S + \delta S$. From the conservation of entropy,

$$\frac{\delta m}{m} = \exp\left(-\frac{\gamma - 1}{\gamma} \frac{\mu \delta S}{\mathcal{R}}\right) - 1. \tag{3}$$

For the sake of simplicity, the ratio of the molecular weight μ to the gas constant \mathcal{R} is set to $\mu/\mathcal{R} = 1$ throughout this paper, with no loss of generality. The total energy δE_{12} released during the advection through the nozzle is calculated in Appendix A:

$$\delta E_{12} = (h_2 - h_1)\delta m. \tag{4}$$

This calculation, which involves no linearization, indicates that the the release of energy during the advection of a localized entropy perturbation is a fundamental process associated to the variation of enthalpy in the flow. δE_{12} corresponds to the sum of the energies of two localized pressure perturbations propagating with and against the stream. According to Eq. (4), the bigger the increase of entropy through the flow, the bigger the release of acoustic energy by the advection of entropy perturbations. In an accretion flow governed by a gravitational potential $\Phi \equiv$ GM/r, the lengthscale of the inhomogeneity of the flow scales like the distance r to the accretor. Consequently there is no region II where the flow is uniform as in Fig. 1. Nevertheless, the time needed by an entropy perturbation to reach a pressure equilibrium with the surrounding gas is of the order of the sound crossing time $\delta l/c$, where δl is the length of the entropy perturbation along the flow. The distance it travels before the pressure equilibrium is reached is of the order of $\mathcal{M}\delta l$, where $\mathcal{M} \equiv v/c$ is the mach number of the flow. The above calculation of δE_{12} is thus relevant for an accretion flow in the region where the length of the perturbation is short enough compared to the scale of the flow inhomogeneities:

$$\mathcal{M}\frac{\delta l}{r} \ll 1. \tag{5}$$

Note that Eq. (4) does not specify the relative amplitudes of the pressure perturbations propagating with and against the stream.

2.2. Acoustic flux released by the advection of an entropy wave

If the entropy perturbation were an extended entropy wave, we expect acoustic waves to be triggered by the enthalpy gradient, by the same process as described in Sect. 2.1. By definition, the acoustic energy of an acoustic wave is the part of the energy which depends (in a quadratic way) only on the linear approximation of this wave (e.g. Lighthill 1978, Chap. 1.3). The flux F^{\pm} of this acoustic energy is defined by:

$$F^{\pm} \equiv \dot{M}_0 c^2 \frac{(1 \pm \mathcal{M})^2}{\mathcal{M}} \left(\frac{\delta p^{\pm}}{\gamma p}\right)^2, \tag{6}$$

where \dot{M}_0 is the mass flux and $\mathcal{M} \equiv v/c$ the Mach number. The index (+) is used to denote the wave propagating in the direction of the flow, (-) otherwise. Any perturbation can be decomposed in the linear approximation onto the acoustic and entropic modes as a sum of a pressure perturbation $\delta p = \delta p^+ + \delta p^-$ and an entropy perturbation δS (e.g. Landau & Lifshitz 1987, Chap. 82). The linear response of the flow to small perturbations is described by the two complex coefficients \mathcal{R}_1 , \mathcal{Q}_1 defined at a position r_1 in the flow as follows

$$\frac{\delta p_1^-}{p_1} = \mathcal{R}_1 \frac{\delta p_1^+}{p_1} + \mathcal{Q}_1 \delta S_1. \tag{7}$$

The coefficient \mathcal{R}_1 is directly related to the refraction of the acoustic flux of an incoming pressure perturbation δp_1^+ by the flow inhomogeneities. Using Eqs. (6) and (7) with $\delta S = 0$, the fraction of refracted acoustic flux is:

$$\frac{F_1^+}{F_1^-} = \left(\frac{1 - \mathcal{M}_1}{1 + \mathcal{M}_1}\right)^2 \mathcal{R}_1^2. \tag{8}$$

If there is no incident acoustic wave $(\delta p_1^+ = 0)$, the acoustic flux F_1^- propagating against the stream is directly related to the amplitude of the incident entropy perturbation, and depend on the coefficient \mathcal{Q}_1 as follows:

$$F_1^- \equiv \dot{M}_0 c_1^2 \frac{(1 - \mathcal{M}_1)^2}{\mathcal{M}_1} \mathcal{Q}_1^2 \left(\frac{\delta S_1}{\gamma}\right)^2.$$
 (9)

Both \mathcal{R}_1 and \mathcal{Q}_1 depend on the frequency ω of the perturbation. An accurate calculation of $\mathcal{R}_1, \mathcal{Q}_1$ in a realistic accretion flow is beyond the scope of the present paper, since it would require solving the full set of linearized Euler equations. This will be done in the particular case of a radial flow in a forthcoming paper (Foglizzo 2000). The frequency dependence of \mathcal{R}_1 can be anticipated by remarking that the refraction is negligible for acoustic wave with a wavelength much shorter than the scale of the inhomogeneities of the flow. In an adiabatic accretion flow, the gravitational potential $\Phi \equiv -GM/r$ is responsible for both the acceleration and the heating of the flow. The lengthscale of the flow inhomogeneities decreases towards the accretor, so that we expect a strong refraction at low frequency and a negligible refraction at high frequency. If the accretion flow is accelerated up to supersonic velocities through a sonic surface, acoustic waves with a high enough frequency to penetrate in the supersonic region cannot be refracted out: a frequency cut-off $\omega_{\rm cut}$ therefore corresponds to the highest frequency above which refraction becomes negligible.

2.3. Estimates of \mathcal{R}_1 , \mathcal{Q}_1 based on the compact nozzle approximation

We build in Appendix B a toy model to obtain rough estimates of the entropic-acoustic coupling in an accretion flow where the mach number increases from $\mathcal{M}_1 \leq 1$ to 1. The refraction point $r_a(\omega)$ of acoustic waves of frequency ω separates the flow into two regions:

- a region of propagation $r \geq r_a$ where both the entropic-acoustic coupling and the acoustic refraction are negligible,

- a region $r \le r_a$ where entropy perturbations are coupled to acoustic waves, and where acoustic waves are refracted.

The propagation of acoustic waves in the first region is easily described using the conservation of their acoustic flux. The region of coupling is described using the "compact nozzle approximation", used for jet nozzles by Marble & Candel (1977). This approximation is valid for perturbations with a long enough wavelength in order to treat the nozzle as a discontinuity in the flow. The formulae obtained by Marble & Candel (1977) are extended in Appendix B to the case of a flow in a potential Φ . In this academic case, the nozzle separates the upstream region characterized by a uniform velocity v_a , mach number $\mathcal{M}_a < 1$ and potential Φ_a , and a downstream region characterized by $v_b, \mathcal{M}_b, \Phi_b$. Here again, the wavelength of the perturbations is assumed to be longer than the size of the nozzle. The compact nozzle approximation enables us to compute the amplitude of the acoustic wave $\delta p_a^-/p_a$ propagating upstream against the current, triggered by the refraction of an incoming acoustic wave $\delta p_a^+/p_a$ or by the advection of an entropy wave δS_a .

The following estimates of $|\mathcal{R}_1|$, $|\mathcal{Q}_1|$ are deduced from Appendix B:

$$|\mathcal{R}_1| \sim \frac{1 + \mathcal{M}_1}{1 - \mathcal{M}_1} \frac{c_{\text{son}}^2 - v_a c_a}{c_{\text{son}}^2 + v_a c_a},$$
 (10)

$$|\mathcal{Q}_1| \sim \frac{\mathcal{M}_1^{\frac{1}{2}} \mathcal{M}_a^{\frac{1}{2}}}{1 - \mathcal{M}_1} \frac{c_a}{c_1} \frac{c_{\text{son}}^2 - c_a^2}{c_{\text{son}}^2 + v_a c_a}.$$
 (11)

Following the argument of Appendix B, the most efficient entropic-acoustic coupling is expected at frequencies close to the refraction cut-off $\omega_{\rm cut}$. The maximum value of $|\mathcal{Q}_1|$ is then of the order of

$$|\mathcal{Q}_1| \sim 0.3 \frac{c_{\text{son}}}{c_1} \text{ if } c_{\text{son}} \gg c_1.$$
 (12)

According to the Bernoulli Eq. (1) with a gravitational potential:

$$c_{\rm son}^2 = 2\frac{\gamma - 1}{\gamma + 1} \left(\frac{GM}{r_{\rm son}} + B \right). \tag{13}$$

The coupling coefficient $|\mathcal{Q}_1|$ deduced from Eqs. (12) and (13) can be very large if the sonic radius $r_{\rm son}$ is close to the accretor, as in the radial accretion of a gas with an adiabatic index γ close to 5/3 (Bondi 1952, Foglizzo & Ruffert 1997). We wish to emphasize the fact that Eq. (12) comes out of a rather idealized toy model where both the refraction of acoustic waves and their coupling to entropy perturbations occur in a localized "compact" region. Nevertheless, we assume it is realistic enough to expect $|\mathcal{Q}_1| \gg 1$ if $c_{\rm son} \gg c_1$.

3. Entropy perturbation produced by a sound wave reaching a shock

The acoustic energy propagating against the flow, released by the processes studied above, would escape far from the accretor if no particular boundary is met. This energy however may feed a cycle if some physical process enables the conversion of acoustic energy into entropy perturbations. A similar cycle occurs in jet nozzles, where sound waves reaching the combustion region perturb the combustion and produce entropy perturbations. Here we focus on the case of a sationary shock satisfying the Rankine-Hugoniot conditions. For the sake of simplicity, we restrict ourselves to the case of a shock in the plane y, z with incident Mach number \mathcal{M}_0 in the x direction. The mach number $\mathcal{M}_{\mathrm{sh}} < 1$ immediately after the shock is related to $\mathcal{M}_0 > 1$ through the classical relation:

$$\mathcal{M}_{\rm sh}^2 = \frac{2 + (\gamma - 1)\mathcal{M}_0^2}{2\gamma \mathcal{M}_0^2 - \gamma + 1} > \frac{\gamma - 1}{2\gamma}.$$
 (14)

Let a sound wave $\delta p_{\rm sh}^-$ propagate against the stream along the x-axis in the subsonic region where the sound speed is $c_{\rm sh}$. The more general case of any angle of incidence is treated in Foglizzo (2000). The incident sound wave perturbs the shock surface and generates both a reflected sound wave $\delta p_{\rm sh}^+$ and an entropy perturbation δS . We define the reflexion coefficient $\mathcal{R}_{\rm sh}$ and the efficiency of entropy production $\mathcal{Q}_{\rm sh}$ as follows:

$$\mathcal{R}_{\rm sh} \equiv \frac{\delta p_{\rm sh}^+}{\delta p_{\rm sh}^-},\tag{15}$$

$$Q_{\rm sh} \equiv \frac{p_{\rm sh}\delta S}{\delta p_{\rm sh}^{-}}.$$
 (16)

A simple calculation in Appendix C, similar to Landau & Lifshitz (1987, chap. 90), shows that $\mathcal{R}_{\rm sh}$ and $\mathcal{Q}_{\rm sh}$ are real functions of $\mathcal{M}_{\rm sh}$ and γ . For a strong shock ($\mathcal{M}_0^2 \gg 2/(\gamma-1)$), the coefficients $\mathcal{R}_{\rm sh}$, $\mathcal{Q}_{\rm sh}$ depend only on the adiabatic index γ :

$$\mathcal{R}_{\rm sh} = -\frac{\gamma^{\frac{1}{2}} - 2^{\frac{1}{2}} (\gamma - 1)^{\frac{1}{2}}}{\gamma^{\frac{1}{2}} + 2^{\frac{1}{2}} (\gamma - 1)^{\frac{1}{2}}},\tag{17}$$

$$Q_{\rm sh} = \frac{2^{\frac{3}{2}}}{(\gamma - 1)^{\frac{1}{2}} \left[\gamma^{\frac{1}{2}} + 2^{\frac{1}{2}} (\gamma - 1)^{\frac{1}{2}} \right]}.$$
 (18)

4. Global instability

At a given frequency ω , let us define τ_+, τ_E as respectively the time of acoustic propagation and the advection time from the shock to the refraction point, and τ_- the time of acoustic propagation from the refraction poin to the shock. $\tau_{AA} \equiv \tau_- + \tau_+$ is the duration of the purely acoustic cycle, while $\tau_{EA} \equiv \tau_- + \tau_E$ is the duration of the entropicacoustic cycle.

4.1. Instability of the entropic-acoustic cycle

A first estimate of the entropic-acoustic instability is obtained by neglecting the effect of the purely acoustic cycle. The adiabatic advection of an entropy perturbation

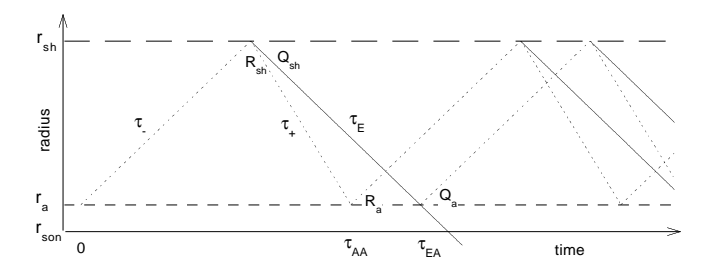


Fig. 2. Schematic trajectories of acoustic (dotted lines) and entropic (full lines) perturbations forming the entropic-acoustic and the purely acoustic parts of the cycle. Acoustic waves are reflected against the shock and refracted by the flow gradients with the respective efficiencies $\mathcal{R}_{\rm sh}$ and \mathcal{R}_a . $r_a > r_{\rm son}$ is the refraction radius. Entropy perturbations are created by the interaction of acoustic waves with the shock with the efficiency $\mathcal{Q}_{\rm sh}$. Their advection triggers outgoing acoustic waves with the efficiency \mathcal{Q}_a . Acoustic propagation times τ_-, τ_+ and entropic advection time τ_E are also illustrated.

of amplitude δS into regions of higher enthalpy produces acoustic waves $\delta p_{\rm sh}^-/p_{\rm sh}$ estimated in Sect. 2. When these acoustic waves reach the shock, new entropy perturbations are created and were estimated in Sect. 3. This leads us to define the global efficiency $\mathcal Q$ of the entropic-acoustic cycle as follows:

$$Q \equiv Q_1 Q_{\rm sh},\tag{19}$$

As for classical problems of modes in e.g. acoustic cavities, the integral phase condition for the existence of an entropic-acoustic mode constrains the real part $\omega_{r,n}$ of its frequency:

$$\omega_{r,n} = \frac{n\pi}{\tau_{EA}},\tag{20}$$

where the integer n must be even if $\mathcal{Q} > 0$ (e.g. in an accretion flow), and odd otherwise (e.g. in a jet nozzle). Note that the duration τ_{EA} of the entropic-acoustic cycle also depends on the frequency through the position of the refraction point. The condition of instability of the entropic-acoustic cycle is $|\mathcal{Q}| > 1$. This leads us to define the global growth (or damping) rate $\omega_{i,n}$ associated to the mode n:

$$\omega_{i,n} = \frac{1}{\tau_{EA}} \log |\mathcal{Q}|. \tag{21}$$

4.2. Which accretion flows are unstable?

On the one hand, we know from Sect. 2.3 that the coefficient $|\mathcal{Q}_1| \gg 1$ if $c_{\rm son} \gg c_{\rm sh}$. On the other hand, we show in Appendix D that the coefficient $\mathcal{Q}_{\rm sh}$ may damp the instability if the shock is too weak. Thus the global efficiency $|\mathcal{Q}|$ exceeds unity for flows such that $c_{\rm son} \gg c_{\rm sh}$ with a strong shock, as in the Bondi-Hoyle accretion with

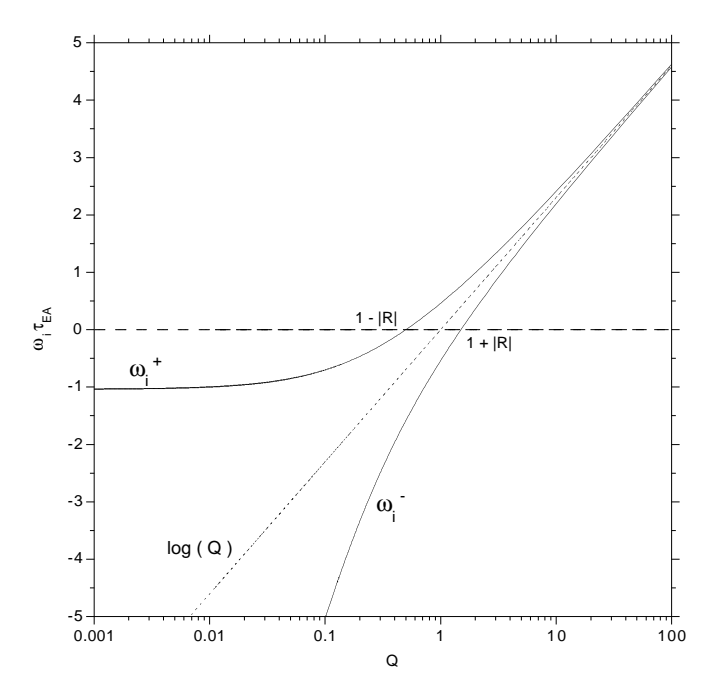


Fig. 3. Growth rate as a function of the global efficiency Q, for $\tau_{AA}/\tau_{EA}=2/3$, $|\mathcal{R}|=0.5$. The dotted line corresponds to the entropic-acoustic cycle alone $\mathcal{R}=0$. The full curves give the upper and lower bounds ω_i^{\pm} of the growth rate when the contribution of the purely acoustic cycle is taken into account. $\omega_i^{\pm}=0$ for $|\mathcal{Q}|=1\mp|\mathcal{R}|$. Eigenmodes are damped for $\omega_i<0$, and unstable for $\omega_i>0$.

 γ close to 5/3 at high Mach number. Following the compact approximation, the frequency of the most unstable mode is close to the refraction cut-off $\omega_{\rm cut}$, which corresponds to a very high order $n_{\rm max}$ if $c_{\rm son} \gg c_{\rm sh}$:

$$n_{\text{max}} \sim \frac{\omega_{\text{cut}} \tau_{EA}}{\pi} \gg 1.$$
 (22)

Eq. (21) indicates that the growth rate depends logarithmically on $|\mathcal{Q}|$, so that the maximum growth rate is always of the order of the inverse of the duration τ_{EA} of a whole entropic-acoustic cycle if $|\mathcal{Q}| \gg 1$. Using Eq. (12),

$$\omega_{i,\text{max}} \sim \frac{1}{\tau_{EA}} \log \frac{c_{\text{son}}}{c_{\text{sh}}}.$$
 (23)

4.3. Contribution of the purely acoustic cycle

A refined estimate of the growth rate and frequency of the instability should take into account the sound waves $\delta p_{\rm sh}^+$ produced at the shock with the efficiency $\mathcal{R}_{\rm sh}$, and their refraction near the sonic radius with the efficiency \mathcal{R}_1 . The global efficiency \mathcal{R} of the purely acoustic cycle is:

$$\mathcal{R} \equiv \mathcal{R}_1 \mathcal{R}_{\rm sh}. \tag{24}$$

The eigenfrequencies must satisfy the following equation, deduced from Eqs. (B.35) and (15-16):

$$Qe^{i\omega\tau_{EA}} + Re^{i\omega\tau_{AA}} = 1. \tag{25}$$

The phase relation between the purely acoustic and the entropic-acoustic cycles is rather complicated (see Eq. E.5). The calculation of the eigenfrequencies requires to know the exact dependence of $\mathcal{Q}, \mathcal{R}, \tau_{EA}, \tau_{AA}$ on the frequency. We show in Appendix E that the growth rate ω_i is bounded to the interval $[\omega_i^-, \omega_i^+]$ satisfying the equation:

$$|\mathcal{Q}|e^{-\omega_i^{\pm}\tau_{EA}} \pm |\mathcal{R}|e^{-\omega_i^{\pm}\tau_{AA}} = 1. \tag{26}$$

The solutions ω_i^{\pm} of this equation are plotted as functions of \mathcal{Q} in Fig. 3. All the modes are unstable for $|\mathcal{Q}| > 1 + |\mathcal{R}|$, while all of them are stable for $|\mathcal{Q}| < 1 - |\mathcal{R}|$. In the range $1 - |\mathcal{R}| < |\mathcal{Q}| < 1 + |\mathcal{R}|$, both stable and unstable modes may be found, depending on the phase of the acoustic cycle. A first order calculation of the contribution of the acoustic cycle when $|\mathcal{R}|/|\mathcal{Q}|^{\tau_{AA}/\tau_{EA}} \ll 1$ leads to:

$$\omega_{r,n} \sim \frac{1}{\tau_{EA}} \left[n\pi - \frac{\mathcal{R}}{|\mathcal{Q}|^{\frac{\tau_{AA}}{\tau_{EA}}}} \sin\left(n\pi \frac{\tau_{AA}}{\tau_{EA}}\right) \right],$$
 (27)

$$\omega_{i,n} \sim \frac{1}{\tau_{EA}} \left[\log |\mathcal{Q}| + \frac{\mathcal{R}}{|\mathcal{Q}|^{\frac{\tau_{AA}}{\tau_{EA}}}} \cos \left(n\pi \frac{\tau_{AA}}{\tau_{EA}} \right) \right],$$
 (28)

where n is even if Q > 0, and odd otherwise. The acoustic cycle can be stabilizing or destabilizing depending on the phase $n\pi\tau_{AA}/\tau_{EA}$. This phase dependence results in a wiggling in the spectrum of the eigenmodes, bounded by ω_i^{\pm} .

4.4. Comparison with the particular case of jet nozzles

The velocity and enthalpy profiles are quite different in a jet nozzle and in an accretion flow. The gas is accelerated in a nozzle at the expense of the enthalpy, whereas gas flowing into a gravitational well $\Phi \equiv -GM/r$ is both accelerated and heated. The limited variation of enthalpy in a nozzle, deduced from the Bernoulli equation with $\Phi \equiv 0$,

$$\frac{c_{\rm son}^2}{c_{\rm sh}^2} = \frac{2 + (\gamma - 1)\mathcal{M}_{\rm sh}^2}{\gamma + 1} < 1,\tag{29}$$

results in a moderate efficiency of the extraction of acoustic energy from the advection of entropy perturbations $(|\mathcal{Q}| < 1)$. Nevertheless, the combustion zone plays a much more active role than the shock described above, since the energy input due to the chemistry of the combustion enables the actual efficiency |Q| to exceed unity. In this respect, the "rumble" instability of ramjets (Abouseif, Keklak & Toong 1984) is different from the entropicacoustic instability described here. Both are based, however, on the cycle of entropic and acoustic perturbations in the subsonic region of the converging flow. In an accretion flow, the efficiency |Q| increases with the frequency up to the refraction cut-off, thus favouring a high frequency instability $(n_{\text{max}} \gg 1)$. By contrast, the most unstable modes in Abouseif, Keklak & Toong (1984) are the low frequency modes.

5. Discussion

We have described how the interplay of entropic and acoustic waves in a subsonic flow between a shock and a sonic point might lead to an entropic-acoustic linear instability. The ingredients for this type of instability are

- (1) an accelerated subsonic flow with a significant increase of sound speed (i.e. of temperature),
- (2) an outer boundary, such as a shock, capable of converting acoustic waves into entropy perturbations.

The stability criterion is directly related to the calculation of a global parameter $\mathcal Q$ describing the coupling of entropy and acoustic waves in the flow. The effect of the purely acoustic cycle is negligible if $|\mathcal Q|\gg 1$, but becomes important near marginal stability (Eq. 26). Although a detailed stability calculation is required for any particular flow topology, general arguments based on the compact nozzle approximation suggest that the entropic-acoustic cycle is potentially unstable if the sound speed at the sonic point significantly exceeds the sound speed immediately after the shock (Eq. 23). The two timescales involved in the entropic-acoustic instability are:

- the period of the most unstable pertubations, of the order of the refraction cut-off,
- the growth time, comparable to the time needed to advect an entropy perturbation from the shock to the sonic radius.

5.1. Astrophysical applications

The entropic-acoustic instability might be at work in several astrophysical situations: as already mentionned in the introduction, the supersonic motion of a compact star in a gas leads to the formation of a bow shock ahead of the accretor. The development of the entropic-acoustic instability in the subsonic region between the shock and the sonic surface is very likely, since $c_{\rm son}/c_{\rm sh}\gg 1$ in these flows (e.g. Ruffert 1996 and references therein). A detailed analysis will be presented in a forthcoming paper.

The acoustic-entropic instability might also be present in some accretion discs. Most stability calculations concerning ADAFs focussed on the *local* thermal stability of the disc (Narayan & Yi 1995, Abramowicz et al. 1995, Kato et al. 1996, 1997, Wu & Li 1996). By contrast, the entropicacoustic instability is a global instability which depends on the outer boundary condition of the flow. The excitation of acoustic waves from an advected entropy perturbation in an ADAF has already been observed in numerical simulations by Manmoto et al. (1996), which include the additional effects of radiative cooling (bremmstrahlung) and viscous heating. Their work was concerned with the time delay problem of Cygnus X-1 and did not involve an outer boundary condition capable of closing the entropicacoustic cycle. Some global disc solutions match a thin disc to an inner ADAF through a shock (Lu, Gu & Yuan 1999). The entropic-acoustic cycle could then occur between this shock and the inner sonic surface. On a larger scale, the gas falling from the Lagrangian point L_1 onto the external radius of an accretion disc might also produce a shock capable of closing the entropic-acoustic cycle. These possible applications deserve a careful analysis which is beyond the scope of the present paper.

5.2. Towards a 3-D description of the instability

Our one-dimensional description assumed that all the outgoing acoustic waves reach the shock, and that all the induced perturbations of entropy reach the sonic surface. Depending on the topology of the flow, possible losses from the entropic-acoustic cycle must be taken into account. In the case of Bondi-Hoyle accretion, outgoing acoustic waves reaching the shock out of the accretion cylinder produce entropy perturbations which will not be accreted, thus diminishing the effective efficiency Q of the cycle. A 3-D description of the entropic-acoustic cycle should also take into account the effect of vorticity perturbations, which are naturally created when an acoustic wave perturbs a shock with a non vanishing angle of incidence. Like the entropy perturbations, the advection of a vorticity perturbation in a converging flow excites acoustic waves (e.g. Howe 1975). Their destabilizing effect will be studied in the particular case of radial accretion (Foglizzo 2000).

5.3. Observable consequences

Understanding the fundamental mechanism of linear instability is only the very first step towards a possible identification of this mechanism in the astrophysical observations. According to our linear description of the entropicacoustic instability, we expect to observe significant variations of the mass accretion rate and displacements of the shock surface as the acoustic energy increases between the shock and the sonic surface. The determination of the spectrum of eigenfrequencies should give valuable informations about the timescale of the most unstable modes. Numerical simulations should be the most direct way to describe the ultimate non-linear development of this instability. We saw that a correct description of the instability requires an accurate propagation of acoustic and entropy waves between the shock and the sonic radius. This could be a serious numerical difficulty for flows where $c_{\rm son} \gg c_{\rm sh}$, since the frequency of the most unstable perturbations could exceed the growth rate by several orders of magnitude. The numerical simulations of Bondi-Hoyle-Lyttleton accretion (e.g. Ruffert 1995) suggest that this instability might lead to some kind of turbulence. This could also be particularly promising if the same mechanism also applies to accretion discs.

Acknowledgements. The authors are grateful to Dr. M. Ruffert for useful discussions, and to an anonymous referee for his constructive comments.

Appendix A: Energy release of a localized perturbation of entropy through a nozzle

We consider in the region I an entropy perturbation δS , corresponding to a perturbation of mass δm initially in pressure equilibrium with the surrounding gas ($\delta p_1 = 0$, $\delta v_1 = 0$). The time scale τ associated to this perturbation of entropy is related to its length l:

$$\tau = \frac{l}{v},\tag{A.1}$$

$$\delta m = \frac{\delta \rho}{\rho} \dot{M}_0 \tau, \tag{A.2}$$

where \dot{M}_0 is the unperturbed mass flux. The entropy perturbation is conserved when advected:

$$\delta S \equiv \frac{1}{\gamma - 1} \log \left(1 + \frac{\delta p}{p} \right) \left(1 + \frac{\delta \rho}{\rho} \right)^{-\gamma}, \tag{A.3}$$

The advected perturbations of density and sound speed ($c^2 \equiv \gamma p/\rho$) follow from Eqs. (A.3):

$$\frac{\delta \rho_1}{\rho_1} = \exp\left(-\frac{\gamma - 1}{\gamma}\delta S\right) - 1,\tag{A.4}$$

$$\frac{\delta c_1^2}{c_1^2} = \exp\left(\frac{\gamma - 1}{\gamma}\delta S\right) - 1. \tag{A.5}$$

The energy flux $F_0 + \delta F_1$ in the perturbation of entropy is defined according to Landau & Lifshitz (1987, Chap. 6), and deduced from Eqs. (1), (A.4) and (A.5):

$$\delta F_1 \equiv (\dot{M}_0 + \delta \dot{M})(B_0 + \delta B) - \dot{M}_0 B_0, \tag{A.6}$$

$$= \dot{M}_0 \left(\frac{v_1^2}{2} + \Phi_1 \right) \left[\exp\left(-\frac{\gamma - 1}{\gamma} \delta S \right) - 1 \right]. \tag{A.7}$$

Replacing the index 1 by the index 2 gives the energy flux $F_0 + \delta F_2$ in the entropy perturbation once it has reached pressure equilibrium with the region II. The total energy δE_{12} released during the advection through the nozzle is therefore:

$$\delta E_{12} \equiv (\delta F_1 - \delta F_2)\tau, \tag{A.8}$$

$$= \dot{M}_0 \tau (h_2 - h_1) \left[\exp \left(-\frac{\gamma - 1}{\gamma} \delta S \right) - 1 \right], \tag{A.9}$$

$$= (h_2 - h_1)\delta m. \tag{A.10}$$

Appendix B: The compact nozzle in a potential $\Phi(r)$

B.1. Conservation equations

The variations $\delta \dot{M}^{\pm}$ and δB^{\pm} of the mass flux \dot{M} and Bernoulli parameter B within a pressure perturbation δp^{\pm} (± 1 depending on the direction of propagation of the perturbation) is to first order:

$$\frac{\delta \dot{M}^{\pm}}{\dot{M}} = \frac{\delta p^{\pm}}{\gamma p} \frac{\mathcal{M} \pm 1}{\mathcal{M}},\tag{B.1}$$

$$\delta B^{\pm} = c^2 (1 \pm \mathcal{M}) \frac{\delta p^{\pm}}{\gamma p}. \tag{B.2}$$

In an entropy perturbation δS in pressure equilibrium with its surrounding, the corresponding variations $\delta \dot{M}^e$ and δB^e are as follows:

$$\frac{\delta \dot{M}^e}{\dot{M}} = -\frac{\gamma - 1}{\gamma} \delta S,\tag{B.3}$$

$$\delta B^e = \frac{c^2}{\gamma} \delta S. \tag{B.4}$$

Writing the conservation of the perturbed entropy, mass flux and Bernoulli parameter across a subsonic nozzle leads to the equations for the subcritical nozzle:

$$\delta S_a = \delta S_b, \tag{B.5}$$

$$\delta \dot{M}_a^+ + \delta \dot{M}_a^- + \delta \dot{M}_a^e = \delta \dot{M}_b^+ + \delta \dot{M}_b^- + \delta \dot{M}_b^e, \tag{B.6}$$

$$\delta B_a^+ + \delta B_a^- + \delta B_a^e = \delta B_b^+ + \delta B_b^- + \delta B_b^e.$$
 (B.7)

The case of a supercritical nozzle requires one more equation describing the effect of perturbations on the sonic surface. The Bernoulli equation can be written at the sonic point r_{son} in a flow tube of entropy S with mass flux \dot{M} and local cross section A_s :

$$B - \Phi(r_{\text{son}}) = \frac{\gamma}{2} \frac{\gamma + 1}{\gamma - 1} \left[\frac{\dot{M}e^S}{\gamma^{\frac{1}{2}} \mathcal{A}_s} \right]^{\frac{2(\gamma - 1)}{\gamma + 1}}.$$
 (B.8)

Differentiating the Bernoulli equation and the mass conservation at the sonic point leads to

$$c_{\rm son}^2 \frac{\delta \mathcal{A}}{\mathcal{A}_s} = \delta \Phi(r_{\rm son}). \tag{B.9}$$

Combining this equation with the differential of Eq. (B.8) provides us with the additional equation required to solve the case of a supercritical nozzle:

$$\frac{\delta \dot{M}}{\dot{M}} + \delta S - \frac{\delta B}{c_{\text{son}}^2} = 0. \tag{B.10}$$

B.2. Incident acoustic wave propagating with the stream

Subcritical nozzle:

$$\frac{\delta p_a^-}{\gamma p_a} = \frac{1 + \mathcal{M}_a}{1 - \mathcal{M}_a} \frac{v_b c_b - v_a c_a}{v_b c_b + v_a c_a} \frac{\delta p_a^+}{\gamma p_a},\tag{B.11}$$

$$\frac{\delta p_b^+}{\gamma p_b} = \frac{1 + \mathcal{M}_a}{1 + \mathcal{M}_b} \frac{2\mathcal{M}_b c_a^2}{v_b c_b + v_a c_a} \frac{\delta p_a^+}{\gamma p_a}.$$
 (B.12)

Supercritical nozzle:

$$\frac{\delta p_a^-}{\gamma p_a} = \frac{1 + \mathcal{M}_a}{1 - \mathcal{M}_a} \frac{c_{\text{son}}^2 - v_a c_a}{c_{\text{son}}^2 + v_a c_a} \frac{\delta p_a^+}{\gamma p_a},\tag{B.13}$$

$$\frac{\delta p_b^+}{\gamma p_b} = \frac{1 + \mathcal{M}_a}{1 + \mathcal{M}_b} \frac{c_a^2}{c_b^2} \frac{c_{\text{son}}^2 + v_b c_b}{c_{\text{son}}^2 + v_a c_a} \frac{\delta p_a^+}{\gamma p_a}, \tag{B.14}$$

$$\frac{\delta p_b^-}{\gamma p_b} = \frac{1 + \mathcal{M}_a}{1 - \mathcal{M}_b} \frac{c_a^2}{c_b^2} \frac{c_{\text{son}}^2 - v_b c_b}{c_{\text{son}}^2 + v_a c_a} \frac{\delta p_a^+}{\gamma p_a}.$$
(B.15)

B.3. Incident entropy perturbation advected with the stream

Subcritical nozzle:

(B.1)
$$\frac{\delta p_a^-}{\gamma p_a} = \frac{\mathcal{M}_a}{1 - \mathcal{M}_a} \frac{c_b^2 - c_a^2}{v_b c_b + v_a c_a} \frac{\delta S}{\gamma},$$
(B.16)

(B.2)
$$\frac{\delta p_b^+}{\gamma p_b} = -\frac{\mathcal{M}_b}{1 + \mathcal{M}_b} \frac{c_b^2 - c_a^2}{v_b c_b + v_a c_a} \frac{\delta S}{\gamma}.$$
 (B.17)

Supercritical nozzle:

$$\frac{\delta p_a^-}{\gamma p_a} = \frac{\mathcal{M}_a}{1 - \mathcal{M}_a} \frac{c_{\text{son}}^2 - c_a^2}{c_{\text{son}}^2 + v_a c_a} \frac{\delta S}{\gamma}, \tag{B.18}$$

$$\frac{\delta p_b^+}{\gamma p_b} = -\frac{c_{\text{son}}^2 - c_a^2}{2(c_{\text{son}}^2 + v_a c_a)} \left[1 + \frac{c_a^2}{c_b^2} \frac{1 + \mathcal{M}_a}{1 + \mathcal{M}_b} \frac{c_b^2 - c_{\text{son}}^2}{c_{\text{son}}^2 - c_a^2} \right] \frac{\delta S}{\gamma}, \tag{B.19}$$

$$\frac{\delta p_b^-}{\gamma p_b} = -\frac{c_{\text{son}}^2 - c_a^2}{2(c_{\text{son}}^2 + v_a c_a)} \left[1 + \frac{c_a^2}{c_b^2} \frac{1 + \mathcal{M}_a}{1 - \mathcal{M}_b} \frac{c_b^2 - c_{\text{son}}^2}{c_{\text{son}}^2 - c_a^2} \right] \frac{\delta S}{\gamma}.$$

B.4. Acoustic flux F_a^- propagating upstream

Since our calculation is based on a linear approximation, we may define efficiencies \mathcal{R}_a , \mathcal{Q}_a of the compact nozzle as follows

$$\frac{\delta p_a^-}{p_a} = \mathcal{R}_a \frac{\delta p_a^+}{p_a} + \mathcal{Q}_a \delta S_a, \tag{B.21}$$

where \mathcal{R}_a , \mathcal{Q}_a are easily deduced from Eqs. (B.11) and (B.16) or Eqs. (B.13) and (B.18), depending on whether the nozzle is subcritical $(\mathcal{M}_b < 1)$, or supercritical $(\mathcal{M}_b > 1)$. The pressure perturbation δp_a^- generated upstream in the case of a supercritical nozzle (Eqs. B.13-B.18) corresponds to the limit of Eqs. (B.11-B.16) when $c_b = c_{\rm son}$, the sound speed at the sonic point. This is consistent with the fact that no information about the fluid properties beyond the sonic point may reach the subsonic region upstream. Note from Eq. (B.18) that the sign of Q_a depends on whether the sound speed of the accelerated gas increases or decreases. The Bernoulli equation implies that $Q_a < 0$ in a classical nozzle $(\Phi \equiv 0)$, while $Q_a > 0$ in an accretion flow. The flux F_a^- of acoustic energy propagating against the stream when an acoustic wave carrying the acoustic flux F_a^+ (with $\delta S=0$) propagates into a supercritial nozzle is deduced from Eqs. (6) and (B.13):

$$\bar{\mathcal{R}}_{a}^{2} \equiv \frac{F_{a}^{-}}{F_{a}^{+}} = \left(\frac{c_{\text{son}}^{2} - v_{a}c_{a}}{c_{\text{son}}^{2} + v_{a}c_{a}}\right)^{2},\tag{B.22}$$

where the refraction efficiency $\bar{\mathcal{R}}_a^2$ is defined in terms of the acoustic energy, while \mathcal{R}_a^2 was defined in Eq. (B.21) in terms of the amplitude of pressure perturbations. It is remarkable that the refraction F_a^-/F_a^+ is independent of the frequency of the incoming acoustic wave. This is true only at low frequency, as long as the compact approximation is satisfied. Refraction is expected to become negligible $(F_a^-/F_a^+\ll 1)$ at high frequency, when the wavelength of an incoming acoustic wave is much shorter than the lengthscale λ of the flow inhomogeneities (i.e. the nozzle size). The refraction cut-off $\omega_{\rm cut}$ is defined as the maximum frequency leading to a significant refraction (e.g. $F_a^-/F_a^+=1/2$).

The flux F_a^- of acoustic energy propagating against the stream when an entropy perturbation δS (with $\delta p^+=0$) is advected into a supercritical nozzle is deduced from Eqs. (6) and (B.18):

$$F_{a}^{-} = \dot{M}_{0} v_{a} c_{a} \left(\frac{c_{\rm son}^{2} - c_{a}^{2}}{c_{\rm son}^{2} + v_{a} c_{a}} \right)^{2} \left(\frac{\delta S}{\gamma} \right)^{2}. \tag{B.23}$$

Here again, the acoustic flux F_a^- is independent of the frequency of the incoming entropy wave, as long as the compact approximation is satisfied. Numerical calculations by Marble &

Candle (1977) show that the efficiency of sound emission from an entropy perturbation also decreases to zero if its wavelength is much shorter than λ . Eq. (B.23) is rewritten using the refraction coefficient $\bar{\mathcal{R}}_a$:

$$F_{a}^{-} = \dot{M}_{0} c_{\rm son}^{2} \bar{\mathcal{R}}_{a}^{2} \left(\frac{1 - \bar{\mathcal{R}}_{a}}{1 + \bar{\mathcal{R}}_{a}} \right) \left(\frac{c_{\rm son}^{2} - c_{a}^{2}}{c_{\rm son}^{2} - c_{a} v_{a}} \right)^{2} \left(\frac{\delta S}{\gamma} \right)^{2}.$$
(B.24)

The ratio $(c_{\rm son}^2-c_a^2)/(c_{\rm son}^2-c_av_a)$ is bounded by

$$\frac{c_{\rm son}^2 - c_a^2}{c_{\rm son}^2 - c_a v_a} \sim 1 \text{ for } c_a \ll c_{\rm son},$$
 (B.25)

$$\sim \left(1 + \frac{\dot{\mathcal{M}}_{\rm son} c_{\rm son}}{2\dot{c}_{\rm son}}\right)^{-1} \text{ for } c_a \sim c_{\rm son},$$
 (B.26)

where $\dot{\mathcal{M}}_{\mathrm{son}}$, \dot{c}_{son} are the derivatives of the mach number and sound speed at the sonic point. Schematically, $\bar{\mathcal{R}}_a$ is constant for $\omega \ll \omega_{\mathrm{cut}}$ and decreases to zero for $\omega \gg \omega_{\mathrm{cut}}$. The maximal value of $\bar{\mathcal{R}}_a^2(1-\bar{\mathcal{R}}_a)/(1+\bar{\mathcal{R}}_a) \sim 0.09$ is reached for $\bar{\mathcal{R}}_a \sim 0.6$, i.e. $v_a c_a \sim c_{\mathrm{son}}^2/4$. We conclude that the acoustic flux propagating against the stream when $F_a^+=0$ is bounded by:

$$F_a^- \le 0.09 \ \dot{M}_0 c_{\rm son}^2 \left(\frac{\delta S}{\gamma}\right)^2. \tag{B.27}$$

B.5. Combination of a slowly accelerated flow and a compact nozzle

Let us build a toy model of a flow $\mathcal{M}_1 \leq \mathcal{M} \leq 1$, especially designed to allow a simple calculation of the interplay of acoustic and entropic perturbations of frequency ω . This flow is composed of:

- a region of propagation $\mathcal{M}_1 \leq \mathcal{M} \leq \mathcal{M}_a$ where both the entropic-acoustic coupling and the acoustic refraction at the frequency ω are negligible, and where the flow is slowly accelerated,
- a compact region $\mathcal{M}_a \leq \mathcal{M} \leq 1$ of coupling, approximated as a supercritical compact nozzle.

The index a notes the entrance of the compact nozzle. These two approximations are compatible if the lengthscale of the flow inhomogeneities is small compared to the wavelength of the perturbations in the compact region, and large compared to this wavelength in the propagation region. The real coefficients $\mathcal{P}_{\pm}, \mathcal{P}_{E}$ describe the amplitude variation of the pressure and entropy perturbations during their propagation between \mathcal{M}_{1} and \mathcal{M}_{a} :

$$\frac{\delta p_a^+}{p_a} \equiv \mathcal{P}_+ \frac{\delta p_1^+}{p_1} e^{i\omega \tau_+}, \tag{B.28}$$

$$\frac{\delta p_1^-}{p_1} \equiv \mathcal{P}_- \frac{\delta p_a^+}{p_a} e^{i\omega\tau_-},\tag{B.29}$$

$$\delta S_a \equiv \mathcal{P}_E \delta S_1 e^{i\omega \tau_E}. \tag{B.30}$$

The values of \mathcal{P}_{\pm} are directly deduced from the conservation of the acoustic flux from \mathcal{M}_a to \mathcal{M}_1 ($F_1^{\pm} \sim F_a^{\pm}$), and \mathcal{P}_E is deduced from the conservation of entropy:

$$\mathcal{P}_{+} = \frac{1 + \mathcal{M}_{1}}{1 + \mathcal{M}_{a}} \frac{\mathcal{M}_{a}^{\frac{1}{2}} c_{1}}{\mathcal{M}_{1}^{\frac{1}{2}} c_{a}}, \tag{B.31}$$

$$\mathcal{P}_{-} = \frac{1 - \mathcal{M}_{a}}{1 - \mathcal{M}_{1}} \frac{\mathcal{M}_{1}^{\frac{1}{2}} c_{a}}{\mathcal{M}_{a}^{\frac{1}{2}} c_{1}}, \tag{B.32}$$

$$\mathcal{P}_E = 1. \tag{B.33}$$

Combining Eqs. (B.21) and (B.31-B.33), we obtain the amplitude δp_1^- of the acoustic waves propagating against the stream at the position \mathcal{M}_1 , as a function of the incident perturbations $\delta p_1^+, \delta S_1$:

$$\mathcal{R}_1 = \mathcal{P}_- \mathcal{P}_+ \mathcal{R}_a e^{i\omega \tau_{AA}} \tag{B.34}$$

$$Q_1 = \mathcal{P}_- \mathcal{P}_E Q_a e^{i\omega \tau_{EA}}. \tag{B.35}$$

Eqs. (10-11) are deduced from Eqs. (B.13), (B.18) and Eqs. (B.31) to (B.33). From the discussion of Sect. B.4, the strongest acoustic flux F_1^- is obtained for $\bar{\mathcal{R}}_a \sim 0.6$

Appendix C: Reflexion of a sound wave at a shock

Consider an adiabatic shock with incident Mach number \mathcal{M}_0 in the x direction. Let a sound wave propagate against the stream in the subsonic region where the sound speed is $c_{\rm sh}$, with wavevector k_- in the frame moving with the fluid. Its frequency ω in the frame stationary with respect to the shock obeys the following dispersion relation (e.g. Landau & Lifschitz, 1986, chap. 68):

$$(\omega - kv_{\rm sh})^2 = c_{\rm sh}^2 k^2. \tag{C.1}$$

The two roots k_{\mp} of this equation correspond to the incident and reflected acoustic waves. The incident acoustic wave perturbs the shock surface and generates both a reflected acoustic wave and an entropy perturbation. The pressure perturbation $\delta p_{\rm sh}$ and the entropy perturbation δS are obtained by writing the jump conditions for an adiabatic shock perturbed with the velocity Δv in the x direction:

$$\frac{\delta p_{\rm sh}}{p_{\rm sh}} = -\frac{4\gamma \mathcal{M}_0^2}{2\gamma \mathcal{M}_0^2 - \gamma + 1} \frac{\Delta v}{v_0},\tag{C.2}$$

$$\frac{\delta v_{\rm sh}}{v_{\rm sh}} = \frac{2(1+\mathcal{M}_0^2)}{2+(\gamma-1)\mathcal{M}_0^2} \frac{\Delta v}{v_0},\tag{C.3}$$

$$\delta S = -\frac{4\gamma (\mathcal{M}_0^2 - 1)^2}{(2 + (\gamma - 1)\mathcal{M}_0^2)(2\gamma \mathcal{M}_0^2 - \gamma + 1)} \frac{\Delta v}{v_0}.$$
 (C.4)

The perturbation is decomposed onto the ingoing and outgoing acoustic waves, and the advected entropy perturbation

$$\delta p_{\rm sh} = \delta p_{\rm sh}^- + \delta p_{\rm sh}^+, \tag{C.5}$$

$$\delta v_{\rm sh} = \delta v_{\rm sh}^- + \delta v_{\rm sh}^+ + \delta v_{\rm sh}^e, \tag{C.6}$$

In addition to the dispersion equation (C.1) for acoustic waves, the acoustic and entropy perturbations are described by:

$$(\omega - k_{\pm})\delta v_{\rm sh}^{\pm} = k_{\pm} \frac{c_{\rm sh}^2}{\gamma} \frac{\delta p_{\rm sh}^{\pm}}{p_{\rm sh}},\tag{C.7}$$

$$\omega = k_e v_{\rm sh},\tag{C.8}$$

$$k_e \delta v_{\rm sh}^e = 0. (C.9)$$

After some algebra with Eqs. (C.1) to (C.9), we obtain:

$$\mathcal{R}_{\rm sh} = -\left(\frac{1 - \mathcal{M}_{\rm sh}}{1 + \mathcal{M}_{\rm sh}}\right)^2 \frac{3 - \gamma - 2(\gamma - 1)\mathcal{M}_{\rm sh}}{3 - \gamma + 2(\gamma - 1)\mathcal{M}_{\rm sh}} < 0, \tag{C.10}$$

$$Q_{\rm sh} = \frac{(1 - \mathcal{M}_{\rm sh})^2}{\mathcal{M}_{\rm sh}} \frac{4}{3 - \gamma + 2(\gamma - 1)\mathcal{M}_{\rm sh}} > 0.$$
 (C.11)

$$\bar{\mathcal{R}}_{\rm sh} \equiv -\left[\frac{1-\mathcal{M}_{\rm sh}}{1+\mathcal{M}_{\rm sh}}\right] \left[\frac{3-\gamma-2(\gamma-1)\mathcal{M}_{\rm sh}}{3-\gamma+2(\gamma-1)\mathcal{M}_{\rm sh}}\right],\tag{C.12}$$

where $\bar{\mathcal{R}}_{\rm sh}^2$ is the reflection coefficient of acoustic waves defined in terms of energy flux rather than amplitudes. For a strong shock, $\bar{\mathcal{R}}_{\rm sh}$ is an increasing function of γ ($\bar{\mathcal{R}}_{\rm sh} \sim -0.14$ for $\gamma = 5/3$):

$$\bar{\mathcal{R}}_{\rm sh} = -\frac{2^{\frac{1}{2}} - \gamma^{\frac{1}{2}} (\gamma - 1)^{\frac{1}{2}}}{2^{\frac{1}{2}} - \gamma^{\frac{1}{2}} (\gamma - 1)^{\frac{1}{2}}}.$$
 (C.13)

Appendix D: Estimates of the global efficiencies \mathcal{Q} and \mathcal{R} based on the compact nozzle approximation

$$\mathcal{R} \equiv \mathcal{P}_{-}\mathcal{P}_{+}\mathcal{R}_{a}\mathcal{R}_{\rm sh},\tag{D.1}$$

$$= \bar{\mathcal{R}}_a \bar{\mathcal{R}}_{\rm sh}. \tag{D.2}$$

 \mathcal{R} depends on the frequency through $\bar{\mathcal{R}}_a$: $\mathcal{R} \sim \bar{\mathcal{R}}_{sh}$ for $\omega \ll \omega_{cut}$, and $\mathcal{R} \sim 0$ for $\omega \gg \omega_{cut}$.

$$Q \equiv \mathcal{P}_{-}\mathcal{P}_{E}Q_{a}Q_{\rm sh},\tag{D.3}$$

$$= \left(\frac{v_a c_a}{v_{\rm sh} c_{\rm sh}}\right)^{\frac{1}{2}} \frac{c_{\rm son}^2 - c_a^2}{c_{\rm son}^2 + v_a c_a} f_{\rm sh},\tag{D.4}$$

$$f_{\rm sh} \equiv \frac{4}{\mathcal{M}_{\rm sh}^{\frac{1}{2}}} \left[\frac{1 - \mathcal{M}_{\rm sh}}{3 - \gamma + 2(\gamma - 1)\mathcal{M}_{\rm sh}} \right]. \tag{D.5}$$

The efficiency Q decreases to zero as $(1 - \mathcal{M}_{\rm sh})$ if the shock is weak. For a strong shock, $f_{\rm sh}$ is a decreasing function of γ $(f_{\rm sh} \sim 1.7 \text{ for } \gamma = 5/3)$:

$$f_{\rm sh} = \left(\frac{2\gamma}{\gamma - 1}\right)^{\frac{1}{4}} \frac{2^{\frac{3}{2}}}{2^{\frac{1}{2}} + \gamma^{\frac{1}{2}}(\gamma - 1)^{\frac{1}{2}}}.$$
 (D.6)

Q is rewritten using the refraction coefficient $\bar{\mathcal{R}}_a$:

$$Q = \frac{c_{\rm son}}{c_{\rm sh}} \bar{\mathcal{R}}_a \left(\frac{1 - \bar{\mathcal{R}}_a}{1 + \bar{\mathcal{R}}_a} \right)^{\frac{1}{2}} \left(\frac{c_{\rm son}^2 - c_a^2}{c_{\rm son}^2 - c_a v_a} \right) f_{\rm sh}. \tag{D.7}$$

Since \mathcal{Q}_a depends strongly on the frequency, the efficiency \mathcal{Q} is a function of ω . Schematically, $\bar{\mathcal{R}}_a \sim 1$ for $\omega \ll \omega_{\rm cut}$, and $\bar{\mathcal{R}}_a \sim 0$ for $\omega \gg \omega_{\rm cut}$, so that \mathcal{Q} reaches its maximum value for a frequency close to the cut-off frequency. In particular $\mathcal{Q}_{\rm max} \gg 1$ if $c_{\rm son} \gg c_{\rm sh}$:

$$f_{\rm sh} \frac{c_{\rm son}}{c_{\rm sh}} > \mathcal{Q}_{\rm max} > 0.3 f_{\rm sh} \left(1 + \frac{\dot{\mathcal{M}}_{\rm son} c_{\rm son}}{2 \dot{c}_{\rm son}} \right)^{-1} \frac{c_{\rm son}}{c_{\rm sh}}.$$
 (D.8)

Appendix E: Contribution of the acoustic cycle

The complex frequency ω is decomposed into its real part ω_r and imaginary part ω_i . Let us introduce the parameter x > 0 and transform the eigenmodes equation as follows:

$$\omega_i \equiv \frac{1}{\tau_{EA}} \log |\mathcal{Q}x|,$$
 (E.1)

$$\frac{\mathcal{Q}}{|\mathcal{Q}|} e^{i\omega_r \tau_{EA}} + x^{1 - \frac{\tau_{AA}}{\tau_{EA}}} \frac{\mathcal{R}}{|\mathcal{Q}|^{\frac{\tau_{AA}}{\tau_{EA}}}} e^{i\omega_r \tau_{AA}} = x. \tag{E.2}$$

The solutions of Eq. (E.2) are bounded by the interval $x_- < x < x_+$, where $x_- < 1 < x_+$ are solutions of the equation:

(C.12)
$$1 \pm x_{\pm}^{1 - \frac{\tau_{AA}}{\tau_{EA}}} \frac{|\mathcal{R}|}{|\mathcal{Q}|^{\frac{\tau_{AA}}{\tau_{EA}}}} = x_{\pm},$$
 (E.3)

from which we obtain Eq. (26) satisfied by the corresponding growth rates ω_i^{\pm} . We deduce from Eqs. (E.1) and (E.3) that

$$\omega_i^{\pm}(|\mathcal{Q}| = 1 \mp |\mathcal{R}|) = 0. \tag{E.4}$$

The real part ω_r must satisfy the following phase equation, deduced from Eq. (E.2):

$$\left[Q\frac{\sin\omega_r(\tau_{AA} - \tau_{EA})}{\sin\omega_r\tau_{AA}}\right]^{\frac{\tau_{AA}}{\tau_{EA}}} = \mathcal{R}\frac{\sin\omega_r(\tau_{EA} - \tau_{AA})}{\sin\omega_r\tau_{EA}}, \quad (E.5)$$

$$x = \frac{Q}{|Q|} \frac{\sin \omega_r (\tau_{AA} - \tau_{EA})}{\sin \omega_r \tau_{AA}}.$$
 (E.6)

If the parameter $|\mathcal{R}|/|\mathcal{Q}|^{\tau_{AA}/\tau_{EA}} \ll 1$, we can estimate the first order contribution of the purely acoustic cycle to the entropic-acoustic instability:

$$x - 1 \sim \frac{\mathcal{R}}{|\mathcal{Q}|^{\frac{\tau_{AA}}{\tau_{EA}}}} \cos \omega_r \tau_{AA}. \tag{E.7}$$

Together with Eq. (E.1-E.2), we obtain Eqs. (27-28).

References

Abouseif G.E., Keklak J.A., Toong T.Y., 1984, Combustion Science and Technology 36, 83

Abramowicz M., Chen X., Kato S., Lasota J.P., Regev O., 1995, ApJ 438, L37

Bondi H., 1952, MNRAS 112, 195

Bondi H., Hoyle F., 1944, MNRAS 104, 273

Candel S.M., 1972, PhD Thesis, California Institute of Technology, Pasadena, California. "Analytical studies of some acoustic problems of jet engines".

De Kool M., Anzer U., 1993, A&A 262, 726

Foglizzo T., Ruffert M., 1997, A&A 320, 342

Foglizzo T., Ruffert M., 1999, A&A 347, 901

Foglizzo T., 2000, in preparation

Fryxell B.A., Taam R.E., 1988, ApJ 335, 862

Fryxell B.A., Taam R.E., McMillan S.L.W., 1987, ApJ 315, $536\,$

Howe M.S., 1975, J. Fluid Mech. 71, 625

Hoyle F., Lyttleton R.A., 1939, Proc. Cam. Phil. Soc. 35, 405

Kato S., Abramowicz M., Chen X., 1996, PASJ 48, 67

Kato S., Yamasaki T., Abramowicz M., Chen X., 1997, PASJ 49, 221

Landau L.D., Lifshitz E.M., 1987, Fluid Mechanics, Vol. 6, Pergamon Press

Lighthill J., 1978, Waves in Fluids, Cambridge University Press
Livio M., 1992, In: Kondo Y., et al. (eds.) IAU Conference on
Evolutionary Processes in Interacting Binary Stars, p. 185
Lu J.-F., Gu W.-M., Yuan F., 1999, ApJ 523, 340

Manmoto T., Takeuchi M., Mineshige S., Matsumoto R., Negoro H., 1996, ApJ 464, L135

Marble F.E. 1973, Symposium on Transportation Noise, Stanford University, March 1973.

Marble F.E., Candel S.M., 1977, Journal of Sound and Vibration 55, 225

Matsuda T., Inoue M., Sawada K., 1987, MNRAS 226,785

Matsuda T., Ishii T., Sekino N., Sawada K., Shima, E., Livio, M., Anzer U., 1992, MNRAS 255, 183

Narayan R., Yi I., 1995, ApJ 452, 710

Ruffert M., 1995, A&AS 113, 133

Ruffert M., 1996, A&A 311, 817

Ruffert M., Arnett D., 1994, ApJ 427, 351

Taam R.E., Fryxell B.A., Brown D.A., 1988, ApJ 331, L117

Wu X., Li Q., 1996, ApJ 469, 645